ACS OMEGA

Open Access

http://pubs.acs.org/journal/acsodf

Article

Development and Analytical Validation of a Surface-Enhanced Raman Scattering Paper Lateral Flow Immunoassay for Detection of the Ubiquitin C-Terminal Hydrolase-L1 Traumatic Brain Injury Biomarker

Weirui Tan, Yingjie Hang, Anyang Wang, Jiacheng Wang, Jane G. Wigginton, Susanne Muehlschlegel, and Nianqiang Wu*

Cite This: *ACS Omega* 2024, 9, 37965−37972

Read Online

ACCESS | Metrics & More | Article Recommendations | Supporting Information

ABSTRACT: Paper lateral flow immunoassays combined with surface-enhanced Raman scattering (SERS) technology have gained increasing attention due to their high sensitivity characteristics resulting from the amplified SERS signals of the plasmon-enhanced optical probes. In contrast to conventional colorimetric lateral flow strips, SERS paper lateral flow strips (SERS-PLFSs) are currently not commercially available for widespread use. Analytical validation is the key step for commercialization. In this work, we have developed a PLFS with a hierarchical SERS probe (gold−silver nanoparticle@Raman reporter@silica) for detection of the US Food and Drug Administration (FDA)-approved traumatic brain injury (TBI) protein biomarker, ubiquitin C-terminal hydrolase-L1 (UCH-L1), in blood plasma samples. Analytical validation has been performed on this SERS-PLFS in terms of the limit of detection (LOD), limit of quantification (LOQ), accuracy, precision, selectivity, and stability. The SERS-PLFS exhibits a reportable range of 0.2−100 ng/mL with a LOD of 0.08 ng/mL toward measurement of UCH-L1 in blood plasma. The SERS-PLFS has been applied to clinical TBI samples. The test results were compared with those from enzyme-linked immunosorbent assay (ELISA), demonstrating a strong correlation between the two analytical methods. This study has important implications in the commercialization of SERS-PLFSs for rapid TBI detection in clinical practice.

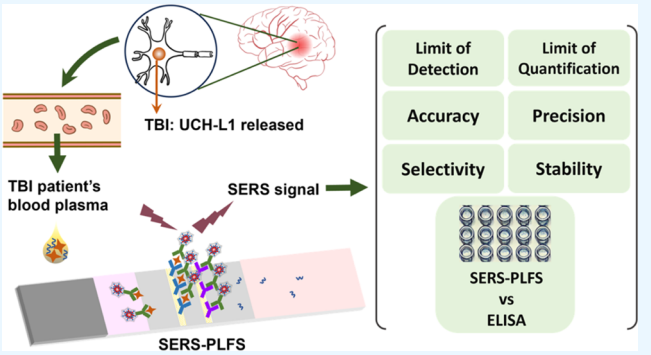

INTRODUCTION

Traumatic brain injury (TBI) poses a substantial public health problem due to its high prevalence and associated long-term disability.[1,2] However, to date, TBI continues to be diagnosed primarily through clinical evaluation and neuroimaging including computed tomography (CT) scans and magnetic resonance imaging (MRI). The recent FDA approval of TBI biomarkers indicates a shift toward using biomarkers for more rapid and accurate TBI diagnoses. Biomarker measurement could greatly improve the triage following traumatic brain injury, ultimately improving patient outcomes and survival rates.[3] Moreover, it could reduce the need for neuroimaging, thereby decreasing potential diagnostic radiation exposure, reducing Emergency Department (ED) wait time and overcrowding, and lowering healthcare expenses.

Protein biomarkers in blood are associated with the pathological processes of TBI, especially reflecting the time course of TBI. Different TBI biomarkers found in the acute, subacute, and chronic stages have been studied to track different phases of TBI.[4,5] Neuron-specific enolase (NSE),[6] UCH-L1,[7] S100 calcium-binding protein B (S-100β),[8] and glial fibrillary acidic protein (GFAP),[9] which elevate within 24 h, have been identified as early diagnostic biomarkers. Among these, UCH-L1 and GFAP are approved by the FDA as characteristic biomarkers for TBI asessment.[10] Different from GFAP, UCH-L1 possesses enzymatic activity[7] and is a neuronal biomarker to specifically reflect acute intracranial lesions.[11] Additionally, UCH-L1 rises earlier and more rapidly than GFAP to peak at 8 h after injury.[12] Therefore, UCH-L1 is more appropriate to rapidly reflect the brain condition after trauma and is considered a pivotal biomarker to respond to TBI-related neurodegeneration. Measurement of UCH-L1 complements the MRI evaluation in TBI diagnosis.[13]

Received: May 16, 2024
Revised: July 22, 2024
Accepted: August 16, 2024
Published: August 26, 2024

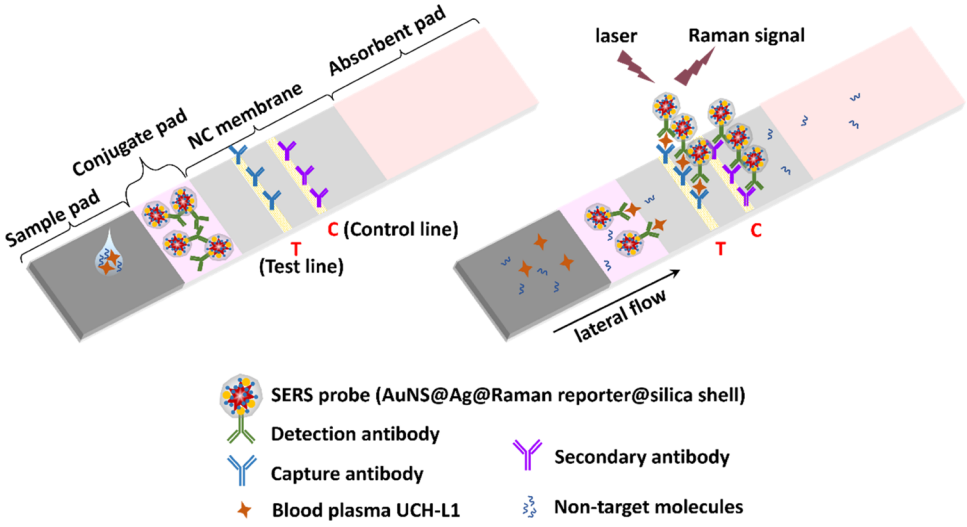

Figure 1. Schematic of the components of the AuNS@Ag SERS-PLFS before and after testing.

Enzyme-linked immunosorbent assay (ELISA) and Western blot are two common techniques for the measurement of these protein biomarkers. Additionally, biosensors based on nanotechnology, e.g., surface plasmon resonance (SPR) and surface-enhanced Raman scattering (SERS), exhibit high sensitivity, but traditionally require tedious operation in a laboratory setting.[14] In contrast, paper lateral flow immunoassays are characterized by low cost, minimized sample volume, and easy operation.[15] However, traditional colorimetric paper lateral flow strips suffer from low sensitivity and severe interference in serum, plasma, and whole blood sample matrices, which limits their ability to accurately detect low concentrations of blood biomarkers. To measure low levels of biomarkers, fluorescence- and SERS-based PLFSs have been developed by taking advantage of their higher sensitivity. For example, Natarajan et al. have developed a fluorescent UCH-L1 PLFS using graphene oxide.[16] Fluorescence signals might be subject to the interference of autofluorescence and even quenched by sample matrices of blood. In contrast, surface-enhanced Raman scattering falls into the near-infrared spectral range and uses the molecular fingerprint peak as the sensing signal, showing great resistance to interference. SERS-PLFSs have emerged with SERS probes, which amplify SERS signals dramatically with plasmonic nanostructures.[17−20] Various nanomaterials have been developed for SERS probes, such as gold nanostars,[6,21] gold nanorods,[22] plasmonic gap-enhanced core−shell nanostructures,[23,24] and bimetal nanostructures.[25] With the optimized SERS probe design, the LOD can be reduced by several orders of magnitude (up to 7) as compared to conventional colorimetric lateral flow assays.[6,21] So far, SERS-PLFSs are in the research and development (R&D) stage in laboratories. Commercial SERS-PLFS products are not yet available. The transition of SERS-PLFSs from laboratory research to bedside application requires several crucial steps including analytical validation, clinical validation, obtaining regulatory approval (e.g., FDA clearance), and the ability to mass-manufacture. The rigorous analytical validation procedures are necessary to validate the reliability, accuracy, and reproducibility of a diagnostic device.

As such, we have designed a SERS-PLFS, in which a bimetal gold-nanostar@silver nanostructure is developed for the SERS probe. The SERS-PLFS is intended to detect UCH-L1 in clinical samples. Analytical validation of the SERS-PLFS is performed by evaluating the LOD, LOQ, accuracy, precision, selectivity, and stability, and then, it is compared with ELISA using plasma samples from patients with acute TBI.

METHODS

Synthesis of AuNS- and AuNS@Ag-Based SERS Probes. Gold nanostar (AuNS), the sandwiched AuNS@4-MBA@silica SERS nanoparticle, and the conjugation of SERS probes with detection antibodies were synthesized following our previous work.[6,26] Preparation of the AuNS@Ag SERS probe from AuNS is illustrated in Figure S1. First, 2.5 mL of AuNS/ethanol with an optical density (OD) of 1.7 measured at the wavelength of 770 nm was mixed with 25 μL of 0.1 M L-ascorbic acid, 5 μL of 0.1 M $AgNO_3$, and 25 μL of 0.1 M NaOH. After keeping overnight, the mixture was washed three times with ethanol, and then AuNS@Ag was dispersed into 2 mL of ethanol. Subsequently, 30 μL of 3 mM 4-MBA was added and stirred for 45 min, followed by the addition of 15 μL of TEOS stock solution. After 15 min, 15 μL of NH_4OH stock solution was introduced and reacted overnight. The reaction solution was washed twice with a mixture of ethanol and DI water in a volume ratio of 1:1. The formed AuNS@Ag@4-MBA@silica solution was suspended into 1 mL of ethanol, followed by adding 20 μL of TEPSA for a 24 h reaction to allow carboxylation. After washing once with ethanol and twice with DI water, carboxyl-group-terminated AuNS@Ag@4-MBA@silica was suspended in 200 μL of DI water. The solution was then activated by 4 μL of 10 mg/mL NHS and EDC, respectively, to form the semistable amine-reactive NHS ester after 1 h of incubation. Next, the detection antibody solution (50 μL, 1 mg/mL monoclonal mouse antihuman UCH-L1 antibody) was added dropwise and incubated at 4 °C for 1 day to thoroughly bind to the silica surface via an amide bond. The resulting AuNS@Ag@4-MBA@silica-detection antibody SERS probes (AuNS@Ag SERS probe) were washed three times with PBS buffer and then stored in 500 μL of probe buffer (Supporting Information) for SERS-PLFS use. The AuNS SERS probe (AuNS@4-MBA@silica-detection Ab) was synthesized following the same procedures from the step of adding 4-MBA (Figure S1b). The information on "Chemicals and Reagents"

https://doi.org/10.1021/acsomega.4c04685
ACS Omega 2024, 9, 37965−37972

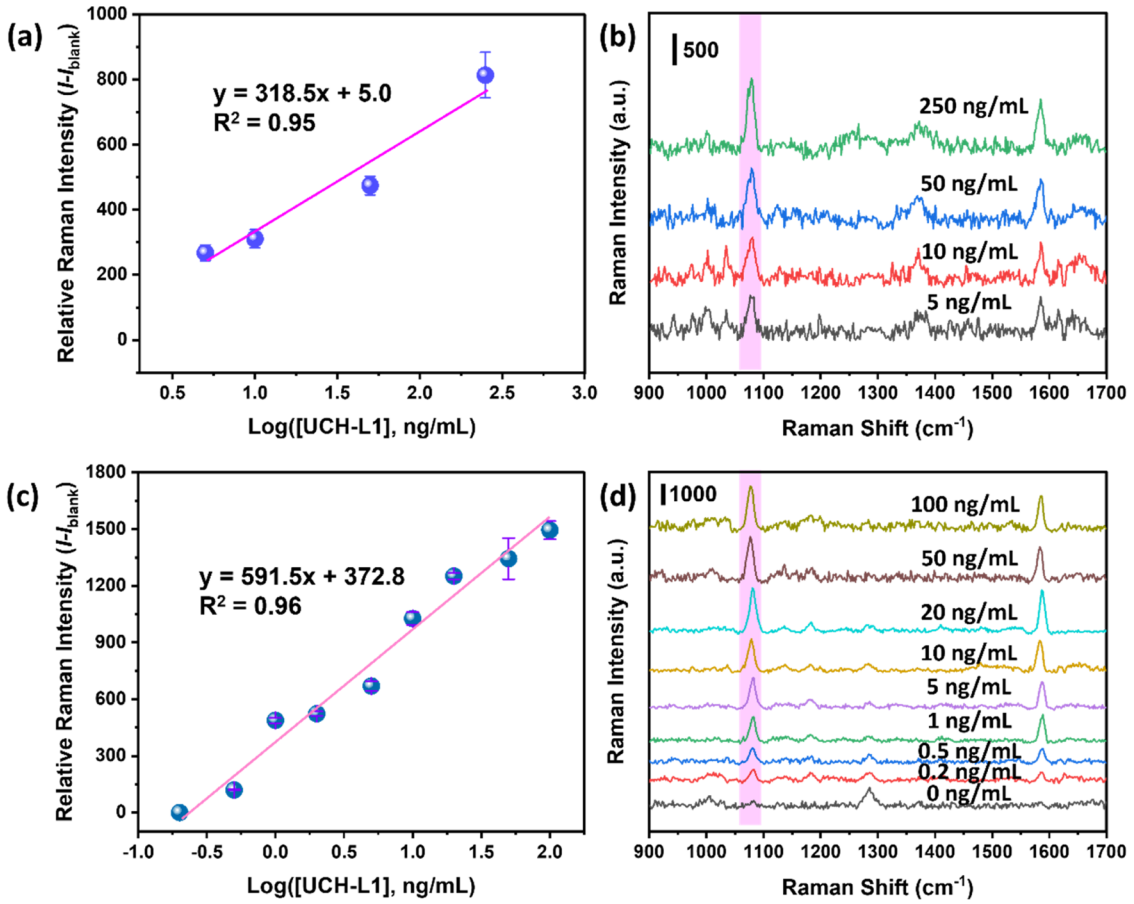

Figure 2. Quantification of the UCH-L1 levels in the mixed plasma (20 vol %) and PBS buffer (80 vol %) solutions. (a) Calibration curve and (b) SERS spectra of the AuNS SERS-PLFS. (c) Calibration curve and (d) SERS spectra of the AuNS@Ag SERS-PLFS, which also includes the SERS spectrum obtained from the control sample of 20% plasma in the absence of spiked UCH-L1.

and the chemicals represented by abbreviations can be found in the Supporting Information.

Preparation of SERS-PLFSs and Colorimetric PLFSs. As shown in Figure 1, the PLFS comprised a sample pad, a conjugate pad, an absorbent pad, and a nitrocellulose (NC) membrane loaded with a test line ("T") and a control line ("C"). The sample pad was pretreated by Tris-HCl buffer.[6] Polyclonal antihuman UCH-L1 antibody from rabbit (0.5 mg/mL, 22 μL) and goat antimouse IgG antibody (1.2 mg/mL, 22 μL) were dispensed once onto a 30 cm long and 25 mm wide NC membrane card by the Autokun dispenser to shape the "T" line and "C" line, respectively. The distance between the two lines was 4 mm. The NC membrane was then incubated in a 37 °C oven for 2 h. To make the paper strip, an NC membrane was overlapped 1−2 mm by an absorbent pad in the downstream side and a conjugate pad in the upstream side, while the conjugate pad was overlapped 1−2 mm by a sample pad. Next, a paper strip in the size of 60 × 3 mm was formed by a cutter. The AuNS- and AuNS@Ag-based SERS-PLFSs were prepared by adding 5.6 μL of the corresponding SERS probe solutions to the conjugate pad. For detection, 80 μL of the sample solution was added to the sample pad, and the fluid flow was driven by capillary force to reach "T" and "C" lines to trigger the sandwich immunoassay. Colorimetric PLFS preparation and operation were conducted in a similar way (details provided in the Supporting Information).

Calibration and LOD. A series of standard UCH-L1 solutions in the mixture of 20% commercial human plasma and 80% PBS buffer were made ranging from 0.2 to 250 ng/mL. Both AuNS- and AuNS@Ag-based SERS-PLFSs were used to calibrate the standard UCH-L1 solutions. All tests were run in triplicate. SERS signals were collected from each strip at 3 points with a portable Raman reader (B&W Tek i-Raman Plus, with a dimension of 16.9 cm × 33.3 cm × 24.2 cm). The SERS peak (intensity of the sensing signal) at 1078 cm^{-1} was plotted as a function of the UCH-L1 concentration. The linear regression curve was generated as the calibration curve. Coefficients of variation (CVs) were calculated for the triplicate measurements of each concentration. The reportable concentration range was determined between the lowest and highest mean concentrations above which the CV was less than 20%. Several standard methods can be used for determining the LOD. For example, the LOD can be calculated as three times the signal-to-noise ratio.[6] In this work, the LOD was calculated following the protocol of the Clinical and Laboratory Standards Institute (eq S1, S2).[27]

RESULTS AND DISCUSSION

AuNS and AuNS@Ag SERS Probes and PLFSs. Both AuNS- and AuNS@Ag-based SERS probes were synthesized as shown in Figure S1 and characterized by TEM (Figure S2). Especially, the bimetallic AuNS@Ag nanoparticles exhibited two separate localized surface plasmon resonance (LSPR) peaks at 641 and 887 nm. After the metallic particles were coated with a silica layer, the two peaks showed a red shift to 720 and 900 nm, respectively, with the short wavelength peak

https://doi.org/10.1021/acsomega.4c04685
ACS Omega 2024, 9, 37965−37972

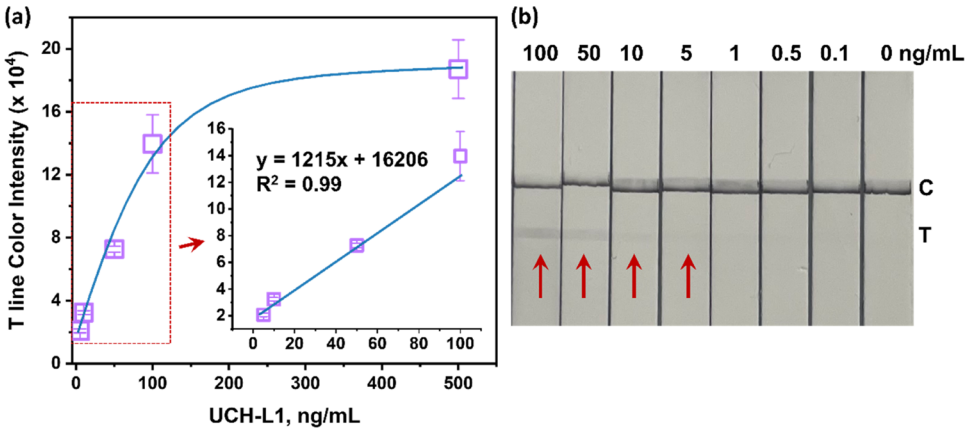

Figure 3. Colorimetric PLFS for calibration of UCH-L1 in the mixed solution of 20% plasma and 80% PBS buffer. (a) Calibration curve of testing UCH-L1 in the range of 5−500 ng/mL. (b) Photos of the colorimetric test results (samples with red arrows can be visualized).

as the primary one (Figure S3). The plasmon peaks can resonate with the excited Raman laser at 785 nm to enhance the SERS signal. The SERS enhancement factors (EFs) of AuNS and AuNS@Ag were calculated as

$$\mathrm{EF} = \frac{I_{\mathrm{SERS}}}{N_{\mathrm{SERS}}} \times \frac{N_{\mathrm{bulk}}}{I_{\mathrm{bulk}}} \quad (1)$$

where I_{bulk} and I_{SERS} are Raman and SERS intensities of the reporter molecules in the bulk solution and on the AuNS or AuNS@Ag substrates, respectively, and N_{bulk} and N_{SERS} are the number of Raman reporter molecules illuminated by a laser beam within the focal volume without and with the SERS substrates, respectively.[28] Our previous work[8] has reported that AuNS achieved a maximum SERS EF ($|E/E_0|^4$) of 10^9 based on the finite-different time-domain (FDTD) simulation results. Based on Figure S4, the SERS signal of 4-MBA on AuNS@Ag is 10-fold higher than that on AuNS in solution, which means that the SERS EF of AuNS@Ag should be much higher. Here, the experimental SERS EF was also calculated. The spot area of 785 nm laser was 2.88 μm^2 with the penetration depth of 6.28 μm,[28] and the density of solid 4-MBA is 1.5 g/cm^3. Each 4-MBA molecule can occupy 0.16 nm^2 and 0.3 nm^2 on AuNS and AuNS@Ag nanoparticles.[29] The number of 4-MBA molecules on AuNS and AuNS@Ag that can be illuminated by a 2.88 μm^2 laser beam was 1.8×10^7 and 9.6×10^6, respectively, while the number of 4-MBA in the bulk solution within the focal volume of the incident lasers was 1.1×10^{11}. Therefore, the calculated SERS EFs for 4-MBA on AuNS and AuNS@Ag were 6.4×10^4 and 1.4×10^6, respectively. In short, AuNS@Ag can achieve 2 orders of magnitude higher than AuNS for SERS enhancement due to more intense "hot spots" on AuNS@Ag (Figure S2b).

Figure 1 shows the components of SERS-PLFSs with the AuNS@Ag@Raman-reporter@silica probes. SERS signals were taken from the "T" line where the analyte (UCH-L1) was sandwiched between the capture antibody and the detection antibody-linked SERS probes (Figures 1 and S5). Figure S6 shows the SERS signals taken from the "T" line after the devices were loaded with 80 μL of 500 ng/mL UCH-L1 in the mixed plasma (20 vol %) and PBS (80 vol %) solution. The AuNS@Ag SERS-PLFS exhibited an SERS signal that was 7.5 times stronger than that of the AuNS SERS-PLFS. The enhanced plasmon coupling in the bimetal Au−Ag nanostructure resulted in a higher enhancement of SERS signals.

LOD and LOQ. Following the protocol of the Clinical and Laboratory Standards Institute,[27] analytical validation was performed on the SERS-PLFS by assessing the LOD, LOQ, and other performance metrics. Figure 2a shows that there existed a linear relationship between the SERS intensity (relative Raman intensity: Raman signals of spiked samples I minus the Raman signal of the blank sample I_{blank}) and the logarithm concentration of UCH-L1 in a range from 5 to 250 ng/mL for the AuNS SERS-PLFS. The linear regression equation was $y = 318.5x + 5.0$ with the relative coefficient (R^2) of 0.95. The LOD was calculated to be 3.4 ng/mL by the equations shown in the Supporting Information. In contrast, for the AuNS@Ag SERS-PLFS, the linear reportable range was 0.2 to 100 ng/mL (Figure 2c), fitted as $y = 591.5x + 372.8$ ($R^2 = 0.96$). The LOD was determined to be 0.08 ng/mL, with a 42.5-fold enhancement in sensitivity compared to that of AuNS. The reduced LOD was attributed to the enhanced LSPR effect of AuNS@Ag, which was stronger than that of AuNS.

The LOQ is defined as the lowest UCH-L1 concentration, which can be quantitatively detected with a CV no larger than 25%. Herein, the LOQ of the AuNS@Ag SERS-PLFS was estimated to be 0.18 ng/mL where the CV was 21.8% (Table S1), as compared to that (LOQ of 0.14 ng/mL) of the ELISA method. The cutoff value of the UCH-L1 concentration in healthy populations is 0.09 ng/mL and peaks at 0.16−0.24 ng/mL in mild TBI patients, while the moderate to severe TBI conditions are reported to have UCH-L1 in various ranges: 1−3.2, 1.7−11.6, 5−8, 20−25, 50−100, and 1.7−11.6 ng/mL.[7] Hence, the AuNS@Ag SERS-PLFS could be used to recognize different severities of TBI conditions by quantifying plasma UCH-L1 concentrations.

For the sake of comparison, the colorimetric PLFS was also fabricated and used to measure UCH-L1 in the 20 vol % plasma + 80 vol % PBS solution. Gold nanoparticles (AuNPs) labeled with anti-UCH-L1 antibodies were adopted as colorimetric probes. The more UCH-L1 molecules were captured on the "T" line, the more AuNPs accumulated, which altered the RGB scale of the winelike color due to the LSPR effect of AuNPs. Figure 3 shows that the color intensity of the "T" line increased with an increase in the UCH-L1 concentration. There existed a linear range from 5 to 100 ng/mL, fitted by $y = 1215x + 16206$ with the relative coefficient (R^2) of 0.99. As shown in Figure 3b, the "T" line can be visualized when the UCH-L1 concentration exceeded 5 ng/

https://doi.org/10.1021/acsomega.4c04685
ACS Omega 2024, 9, 37965−37972

Table 1. Intra-Assay and Interassay Accuracy and Precision of SERS-PLFSs for Testing Positive Control UCH-L1 Plasma Samples

		plasma UCH-L1, ng/mL		
		0.2	2.5	10
		intra-assay		
mean ± SD		0.19 ± 0.04	2.87 ± 0.37	9.48 ± 0.99
accuracy, error %		4.7	−14.8	5.2
precision, CV %		19.2	13.0	10.5
		interassay		
batch 1	mean ± SD	0.18 ± 0.04	2.04 ± 0.12	9.97 ± 0.21
	accuracy, error %	12.3	18.5	0.3
	precision, CV %	22.4	6.1	2.1
batch 2	mean ± SD	0.22 ± 0.05	2.51 ± 0.01	9.43 ± 1.68
	accuracy, error %	−11.8	−0.3	5.7
	precision, CV %	20.5	0.5	17.8
batch 3	mean ± SD	0.16 ± 0.03	2.89 ± 0.05	10.99 ± 2.14
	accuracy, error %	18.3	−15.6	−9.9
	precision, CV %	16.7	1.6	19.5
total	mean ± SD	0.19 ± 0.03	2.48 ± 0.43	10.13 ± 0.79
	accuracy, error %	6.3	0.9	−1.3
	precision, CV %	17.0	17.3	7.8

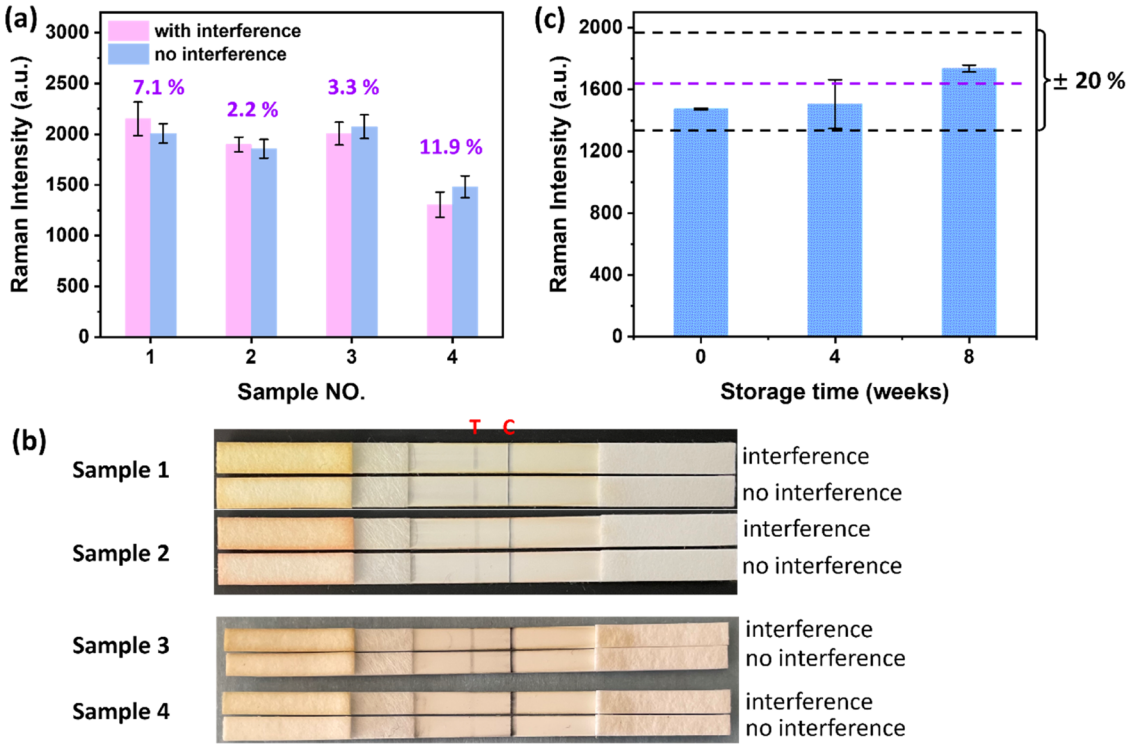

Figure 4. (a) Interference tolerance study of the AuNS@Ag SERS-PLFS for UCH-L1 detection in the presence of interfering components of 1.2 mg/dL bilirubin, 30 mg/dL hemoglobin, and 150 mg/dL triglyceride in the plasma sample matrix and (b) optical photos. (c) Stability of antibodies on the SERS-PLFS stored at −20 °C.

mL. The LOD was estimated to be 4.1 ng/mL, which was 2 orders of magnitude higher than that of the AuNS@Ag SERS-PLFS. Therefore, the colorimetric PLFS cannot be used to detect various severities of TBI due to the insufficient sensitivity.

The state-of-the-art PLFS based on different technologies for detecting TBI biomarkers is also summarized in Table S2. It shows that the AuNS@Ag SERS-PLFS is the first one reported to measure UCH-L1 in blood plasma and can achieve a LOD (0.08 ng/mL) lower than the cutoff value (0.1 ng/mL). Most importantly, analytical validation of SERS-PLFSs is for the first time reported here.

Accuracy and Precision. Accuracy reflects the systematic error, and precision reveals the degree of reproducibility, both of which were calculated based on eq S3−S5. Here, intra- and interassay accuracies and precisions were carried out by testing various plasma UCH-L1 concentrations covering three levels (from "close to LOQ" to high UCH-L1 levels). Intra-assay is a measure of the variance between data points within an assay, meaning that sample replicates were run within the same

https://doi.org/10.1021/acsomega.4c04685
ACS Omega 2024, 9, 37965−37972

batch. Interassay refers to the variance between runs of sample replicates on three different batches that can be used to assess batch-to-batch consistency. Accuracy is acceptable with the systematic error within ±20% (±25% at LOQ) and the CV of precision should not exceed 20% (25% at LOQ).[30] Table 1 shows the systematic error % was ranging from −14.8 to 5.2 for intra-assay and −15.6 to 18.5 for interassay, not exceeding ±20%. The precision CV % varied from 10.5 to 19.2 for intra-assay. For interassay, the CV % was from 0.5 to 19.5 for the two quality control samples (2.5 and 10 ng/mL), while for the "close to LOQ" sample (0.2 ng/mL), the highest CV % was 22.4, not exceeding 25%.

Selectivity and Stability. Nontarget molecules, coexisting in blood plasma samples, might interfere with the UCH-L1 measurement, which might make the SERS-PLFS show cross-sensitivity toward the nontarget molecules. Hence, the selectivity of the AuNS@Ag SERS-PLFS was evaluated. Four random TBI patient blood plasma samples (Figure 4a,b) with unknown UCH-L1 concentrations were half diluted with PBS buffer and were split into two groups: the control group ("no interference") and the test group ("with interference") spiked with 1.2 mg/dL bilirubin, 30 mg/dL hemoglobin, and 150 mg/dL triglyceride (all are the upper limit values in healthy adult blood plasma).[31−33] The SERS signal difference (%I) is calculated by

$$\%I = \frac{\overline{I}_{\text{interference}} - \overline{I}_{\text{no interference}}}{\overline{I}_{\text{no interference}}} \times 100\% \quad (2)$$

which was in the range of 2.2−11.9% (Figure 4a). This indicates that the AuNS@Ag SERS-PLFS exhibited excellent selectivity toward UCH-L1 identification in plasma sample matrices.

The storage stability of the SERS-PLFS was also evaluated (Supporting Information). The SERS-PLFSs were stored at −20 °C, and the immunoassay activity of antibodies on the PLFS was tested at intervals of the storage time. Figure 4c shows that the SERS-PLFS retained excellent activity toward UCH-L1 detection in the eighth week, and the SERS signal varied less than ±20% for all PLFSs after different storage durations.

Clinical Sample Detection with SERS-PLFS and ELISA Methods. Both AuNS@Ag SERS-PLFS and ELISA methods were used to measure 115 blood plasma samples (99 TBI patient samples and 16 quality control samples). Figure 5a shows the Bland−Altman plot, which identified the systematic deviations between SERS-PLFS and ELISA measurements (i.e., fixed bias). The standard deviation measured the fluctuation around the mean difference and reflected the imprecision of the measurements. The dashed lines at ±1.96 standard deviation (SD) from the mean difference denoted the 95% limits of agreement, indicating that assuming normally distributed differences, 95% of measurement differences between the two methods fell within this range. The analysis revealed that 111 samples (depicted as red dots) fell within the 95% confidence interval, suggesting a statistically robust agreement between SERS-PLFS and ELISA measurements. Linear regression analysis also indicates that the SERS-PLFS test results were strongly correlated with the ELISA results (Figure 5b), giving a fitting formula: $y = 1.12x - 0.03$ (95% CI: 0.90−0.95) with a Pearson correlation coefficient (R) of 0.93. It is noticed that four points, as shown in Figure 5a (marked with black dots) and Figure 5b (marked with black circles), led to a much higher difference from other points, which was ascribed to the abnormal conditions of the samples that suffered from severe hemolysis, suspended solids (e.g., fat) with a higher viscosity, and other issues.

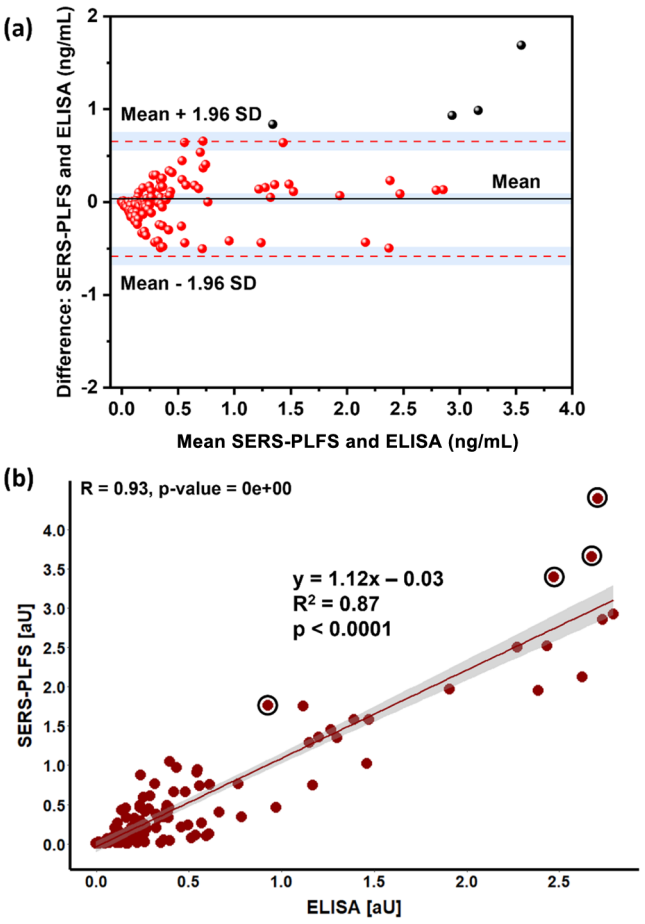

Figure 5. Comparison between ELISA and SERS-PLFS methods in testing TBI blood plasma samples. (a) Bland−Altman plots for each sample indicate differences between the two assays. Points in red color between the dashed lines illustrate the sample pairs within ±1.96 SD, while the black points outside the acceptable region represent greater deviations. (b) Linear regression analysis evaluating the Pearson correlation of test results obtained for TBI blood plasma samples (n = 115) by the SERS-PLFS method with those obtained by ELISA.

CONCLUSIONS

A SERS-PLFS with a bimetallic AuNS@Ag nanostructure SERS probe has been developed for the detection of the TBI biomarker UCH-L1. The current SERS detection system with a portable reader can be used in emergency departments. The AuNS@Ag SERS-PLFS exhibited a LOD of 0.08 ng/mL toward UCH-L1 measurement in blood plasma, which showed better sensitivity than the AuNS SERS-PLFS and colorimetric PLFS. This was attributed to the excellent SERS enhancement capability of the AuNS@Ag SERS probe resulting from the plasmonic coupling effect. The AuNS@Ag SERS-PLFS displayed a reportable range of 0.2−100 ng/mL for plasma UCH-L1 detection, consistent with various severities of TBI. Comprehensive analytical validation was performed on the AuNS@Ag SERS-PLFS to evaluate the sensing performance. The LOQ was estimated to be 0.18 ng/mL with a CV of

https://doi.org/10.1021/acsomega.4c04685
ACS Omega 2024, 9, 37965−37972

21.8%, within the acceptance value (≤25%). Both intra- and interassay accuracies and precisions were assessed, with the calculated systematic error within ±20% and the CV not exceeding 20% for quality control samples and 25% for the LOQ test, respectively. The selectivity study showed that the SERS signal difference between the control and spiked samples was within an acceptable range (2.2−11.9%) for interference tolerance. The AuNS@Ag SERS-PLFS was used to detect plasma samples taken from patients with TBI. The test results of the SERS-PLFS exhibited a strong correlation with those of ELISA. A combination of SERS with paper lateral flow immunoassay technology holds great potential to overcome the sensitivity barrier and enable the rapid quantification of UCH-L1 biomarker levels. Analytical validation is essential for the commercialization of SERS-PLFSs, which is significant for the rapid, accurate, inexpensive, portable, and technically simple screening of TBI.

■ ASSOCIATED CONTENT

Supporting Information

The Supporting Information is available free of charge at https://pubs.acs.org/doi/10.1021/acsomega.4c04685.

Reagents and preparation of the probe buffer and the colorimetric probe; LOD, accuracy, and precision calculation methods; selectivity, storage stability, and clinical patient sample collection procedures; schematic of AuNS@Ag and AuNS SERS probe synthesis; TEM images, UV−vis spectra, and SERS signals of two types of probes in solution and on PLFSs; schematic figure of AuNS-based SERS-PLFS; and tables of LOQ, CV, and PLFS techniques for measuring TBI biomarkers (PDF)

■ AUTHOR INFORMATION

Corresponding Author

Nianqiang Wu − *Department of Chemical Engineering, University of Massachusetts Amherst, Amherst, Massachusetts 01002, United States;* orcid.org/0000-0002-8888-2444; Email: nianqiangwu@umass.edu

Authors

Weirui Tan − *Department of Chemical Engineering, University of Massachusetts Amherst, Amherst, Massachusetts 01002, United States;* orcid.org/0000-0001-8773-5656

Yingjie Hang − *Department of Chemical Engineering, University of Massachusetts Amherst, Amherst, Massachusetts 01002, United States*

Anyang Wang − *Department of Chemical Engineering, University of Massachusetts Amherst, Amherst, Massachusetts 01002, United States*

Jiacheng Wang − *Department of Chemical Engineering, University of Massachusetts Amherst, Amherst, Massachusetts 01002, United States;* orcid.org/0000-0002-7948-8525

Jane G. Wigginton − *Center for BrainHealth and Texas Biomedical Device Center, The University of Texas at Dallas, Richardson, Texas 75080, United States*

Susanne Muehlschlegel − *Departments of Neurology and Anesthesiology/Critical Care Medicine, Johns Hopkins University School of Medicine, Baltimore, Maryland 21287, United States; Department of Neurology, University of Massachusetts Chan Medical School, Worcester, Massachusetts 02655, United States*

Complete contact information is available at: https://pubs.acs.org/10.1021/acsomega.4c04685

Notes

The authors declare no competing financial interest.

■ ACKNOWLEDGMENTS

This work was partially supported by the National Institute of Neurological Disorders and Stroke (NINDS) of the National Institutes of Health (1U01NS119647-01). The content is solely the responsibility of the authors and does not necessarily represent the official views of the National Institutes of Health.

■ REFERENCES

(1) Galgano, M.; Toshkezi, G.; Qiu, X.; Russell, T.; Chin, L.; Zhao, L.-R. Traumatic brain injury: current treatment strategies and future endeavors. *Cell Transplantation* **2017**, *26* (7), 1118−1130.

(2) Haarbauer-Krupa, J.; Pugh, M. J.; Prager, E. M.; Harmon, N.; Wolfe, J.; Yaffe, K. Epidemiology of chronic effects of traumatic brain injury. *J. Neurotrauma* **2021**, *38* (23), 3235−3247.

(3) Thelin, E.; Al Nimer, F.; Frostell, A.; Zetterberg, H.; Blennow, K.; Nyström, H.; Svensson, M.; Bellander, B.-M.; Piehl, F.; Nelson, D. W. A serum protein biomarker panel improves outcome prediction in human traumatic brain injury. *J. Neurotrauma* **2019**, *36* (20), 2850−2862.

(4) Wang, K. K.; Yang, Z.; Zhu, T.; Shi, Y.; Rubenstein, R.; Tyndall, J. A.; Manley, G. T. An update on diagnostic and prognostic biomarkers for traumatic brain injury. *Expert Rev. Mol. Diagn.* **2018**, *18* (2), 165−180.

(5) Maas, A. I. R.; Menon, D. K.; Manley, G. T.; Abrams, M.; Åkerlund, C.; Andelic, N.; Aries, M.; Bashford, T.; Bell, M. J.; Bodien, Y. G. J. T. L. N.; et al. Traumatic brain injury: progress and challenges in prevention, clinical care, and research. *Lancet Neurol.* **2022**, *21* (11), 1004−1060.

(6) Gao, X.; Zheng, P.; Kasani, S.; Wu, S.; Yang, F.; Lewis, S.; Nayeem, S.; Engler-Chiurazzi, E. B.; Wigginton, J. G.; Simpkins, J. W.; Wu, N. Paper-Based Surface-Enhanced Raman Scattering Lateral Flow Strip for Detection of Neuron-Specific Enolase in Blood Plasma. *Anal. Chem.* **2017**, *89* (18), 10104−10110.

(7) Singh, G. P.; Nigam, R.; Tomar, G. S.; Monisha, M.; Bhoi, S. K.; S, A.; Sengar, K.; Akula, D.; Panta, P.; Anindya, R. Early and rapid detection of UCHL1 in the serum of brain-trauma patients: a novel gold nanoparticle-based method for diagnosing the severity of brain injury. *Analyst* **2018**, *143* (14), 3366−3373.

(8) Gao, X.; Boryczka, J.; Zheng, P.; Kasani, S.; Yang, F.; Engler-Chiurazzi, E. B.; Simpkins, J. W.; Wigginton, J. G.; Wu, N. A "hot Spot"-Enhanced paper lateral flow assay for ultrasensitive detection of traumatic brain injury biomarker S-100beta in blood plasma. *Biosens. Bioelectron.* **2021**, *177*, No. 112967.

(9) Zheng, P.; Kasani, S.; Tan, W.; Boryczka, J.; Gao, X.; Yang, F.; Wu, N. Plasmon-enhanced near-infrared fluorescence detection of traumatic brain injury biomarker glial fibrillary acidic protein in blood plasma. *Anal. Chim. Acta* **2022**, *1203*, No. 339721.

(10) Korley, F. K.; Datwyler, S. A.; Jain, S.; Sun, X.; Beligere, G.; Chandran, R.; Marino, J. A.; McQuiston, B.; Zhang, H.; Caudle, K. L.; et al. Comparison of GFAP and UCH-L1 measurements from two prototype assays: the Abbott i-STAT and ARCHITECT assays. *Neurotrauma Rep.* **2021**, *2* (1), 193−199.

(11) Nishimura, K.; Cordeiro, J. G.; Ahmed, A. I.; Yokobori, S.; Gajavelli, S. Advances in traumatic brain injury biomarkers. *Cureus* **2022**, *14* (4), No. e23804.

(12) Papa, L.; Brophy, G. M.; Welch, R. D.; Lewis, L. M.; Braga, C. F.; Tan, C. N.; Ameli, N. J.; Lopez, M. A.; Haeussler, C. A.; Mendez Giordano, D. I.; et al. Time Course and Diagnostic Accuracy of Glial and Neuronal Blood Biomarkers GFAP and UCH-L1 in a Large Cohort of Trauma Patients With and Without Mild Traumatic Brain Injury. *JAMA Neurol.* **2016**, *73* (5), 551−560.

(13) Kou, Z.; Gattu, R.; Kobeissy, F.; Welch, R. D.; O'Neil, B. J.; Woodard, J. L.; Ayaz, S. I.; Kulek, A.; Kas-Shamoun, R.; Mika, V.;

et al. Combining biochemical and imaging markers to improve diagnosis and characterization of mild traumatic brain injury in the acute setting: results from a pilot study. *PLoS One* **2013**, *8* (11), No. e80296.
(14) Borumand, M. R.; Babaloii, F.; Mirmotahari, S. A.; Maghsoudi, A. S.; Torabi, R.; Mojtahedzadeh, M.; Norouzi, P.; Rad-Malekshahi, M.; Javar, H. A.; Hassani, S. Recent trends and innovations in biosensors development for biomarkers towards monitoring traumatic brain injury. *Biosens. Bioelectron: X* **2022**, *12*, 100247.
(15) Liu, Y.; Zhan, L.; Qin, Z.; Sackrison, J.; Bischof, J. C. Ultrasensitive and highly specific lateral flow assays for point-of-care diagnosis. *ACS Nano* **2021**, *15* (3), 3593−3611.
(16) Natarajan, S.; Joseph, J.; Prazeres, D. M. F. Graphene oxide coatings enhance fluorescence signals in a lateral flow immunoassay for the detection of UCH-L1, a marker for trauma brain injury. *Sens. Actuators B Chem.* **2023**, *393*, 134336.
(17) Hwang, J.; Lee, S.; Choo, J. Application of a SERS-based lateral flow immunoassay strip for the rapid and sensitive detection of staphylococcal enterotoxin B. *Nanoscale* **2016**, *8* (22), 11418−11425.
(18) Chen, S.; Meng, L.; Wang, L.; Huang, X.; Ali, S.; Chen, X.; Yu, M.; Yi, M.; Li, L.; Chen, X.; et al. SERS-based lateral flow immunoassay for sensitive and simultaneous detection of anti-SARS-CoV-2 IgM and IgG antibodies by using gap-enhanced Raman nanotags. *Sens Actuators B Chem.* **2021**, *348*, No. 130706.
(19) Lu, M.; Joung, Y.; Jeon, C. S.; Kim, S.; Yong, D.; Jang, H.; Pyun, S. H.; Kang, T.; Choo, J. Dual-mode SERS-based lateral flow assay strips for simultaneous diagnosis of SARS-CoV-2 and influenza a virus. *Nano Converg.* **2022**, *9* (1), 39.
(20) Sloan-Dennison, S.; O'Connor, E.; Dear, J. W.; Graham, D.; Faulds, K. Towards quantitative point of care detection using SERS lateral flow immunoassays. *Anal. Bioanal. Chem.* **2022**, *414* (16), 4541−4549.
(21) Srivastav, S.; Dankov, A.; Adanalic, M.; Grzeschik, R.; Tran, V.; Pagel-Wieder, S.; Gessler, F.; Spreitzer, I.; Scholz, T.; Schnierle, B.; et al. Rapid and Sensitive SERS-Based Lateral Flow Test for SARS-CoV2-Specific IgM/IgG Antibodies. *Anal. Chem.* **2021**, *93* (36), 12391−12399.
(22) Yu, Q.; Zhang, J.; Qiu, W.; Li, K.; Qian, L.; Zhang, X.; Liu, G. Gold nanorods-based lateral flow biosensors for sensitive detection of nucleic acids. *Microchim Acta* **2021**, *188* (4), 133.
(23) Tian, R.; Ren, Y.; Wang, T.; Cao, J.; Li, J.; Deng, A. A SERS-based lateral flow immunochromatographic assay using Raman reporter mediated-gap AuNR@Au nanoparticles as the substrate for the detection of enrofloxacin in food samples. *Anal. Chim. Acta* **2023**, *1257*, No. 341152.
(24) Khlebtsov, B. N.; Bratashov, D. N.; Byzova, N. A.; Dzantiev, B. B.; Khlebtsov, N. G. SERS-based lateral flow immunoassay of troponin I by using gap-enhanced Raman tags. *Nano Res.* **2019**, *12* (2), 413−420.
(25) Liu, B.; Zheng, S.; Liu, Q.; Gao, B.; Zhao, X.; Sun, F. SERS-based lateral flow immunoassay strip for ultrasensitive and quantitative detection of acrosomal protein SP10. *Microchem. J.* **2022**, *175*, 107191.
(26) Li, M.; Cushing, S. K.; Zhang, J.; Suri, S.; Evans, R.; Petros, W. P.; Gibson, L. F.; Ma, D.; Liu, Y.; Wu, N. Three-dimensional hierarchical plasmonic nano-architecture enhanced surface-enhanced Raman scattering immunosensor for cancer biomarker detection in blood plasma. *ACS Nano* **2013**, *7* (6), 4967−4976.
(27) Armbruster, D. A.; Pry, T. Limit of blank, limit of detection and limit of quantitation. *Clin. Biochem. Rev.* **2008**, *29* (Suppl1), S49.
(28) Pan, X.; Li, L.; Lin, H.; Tan, J.; Wang, H.; Liao, M.; Chen, C.; Shan, B.; Chen, Y.; Li, M. A graphene oxide-gold nanostar hybrid based-paper biosensor for label-free SERS detection of serum bilirubin for diagnosis of jaundice. *Biosens. Bioelectron.* **2019**, *145*, No. 111713.
(29) Zhu, S.; Fan, C.; Wang, J.; He, J.; Liang, E. Surface-enhanced Raman scattering of 4-mercaptobenzoic acid and hemoglobin adsorbed on self-assembled Ag monolayer films with different shapes. *Appl. Phys. A: Mater. Sci. Process.* **2014**, *117* (3), 1075−1083.
(30) FDA, U. S.. *Bioanalytical Method Validation Guidance For Industry*; US Department of Health and Human Services Food and Drug Administration Center for Drug Evaluation and Research and Center for Veterinary Medicine, 2018.
(31) Tan, W.; Zhang, L.; Doery, J. C.; Shen, W. Three-dimensional microfluidic tape-paper-based sensing device for blood total bilirubin measurement in jaundiced neonates. *Lab Chip* **2020**, *20* (2), 394−404.
(32) Tan, W.; Zhang, L.; Doery, J. C.; Shen, W. Study of paper-based assaying system for diagnosis of total serum bilirubin by colorimetric diazotization method. *Sens. Actuators B: Chem.* **2020**, *305*, No. 127448.
(33) Fan, W.; Philip, S.; Granowitz, C.; Toth, P. P.; Wong, N. D. Prevalence of US adults with triglycerides≥ 150 mg/dl: NHANES 2007−2014. *Cardiol Ther* **2020**, *9*, 207−213.

https://doi.org/10.1021/acsomega.4c04685
ACS Omega 2024, 9, 37965−37972